### Title

Bifunctional Catalysis Prevents Inhibition in Reversible-Deactivation Ring-Opening Copolymerizations of Epoxides and Cyclic Anhydrides




### Journal

Journal of the American Chemical Society, 142(47)

### ISSN

0002-7863



### Authors

Lidston, Claire AL
Abel, Brooks A
Coates, Geoffrey W



### Publication Date

2020-11-25

### DOI

10.1021/jacs.0c10014

Peer reviewed

JACS
JOURNAL OF THE AMERICAN CHEMICAL SOCIETY
pubs.acs.org/JACS
Article

# Bifunctional Catalysis Prevents Inhibition in Reversible-Deactivation Ring-Opening Copolymerizations of Epoxides and Cyclic Anhydrides

Claire A. L. Lidston,[#] Brooks A. Abel,[#] and Geoffrey W. Coates*

Cite This: *J. Am. Chem. Soc.* 2020, 142, 20161–20169
Read Online



**ABSTRACT:** Reversible-deactivation chain transfer is a viable strategy to increase the catalytic efficiency of ring-opening polymerizations, such as the alternating copolymerization of epoxides and cyclic anhydrides. In conjunction with the catalyst, protic chain transfer agents (CTAs) initiate polymerization and facilitate rapid proton transfer between active and dormant chains. Functional-group-tolerant Lewis acid catalysts are therefore required to successfully apply protic CTAs in reversible-deactivation ring-opening copolymerizations (RD-ROCOP), yet the predominant binary Lewis acid catalyst/nucleophilic cocatalyst systems suffer lower polymerization rates when used with protic CTAs. New mechanistic insight into the inhibition pathways reveals that the alcohol chain ends compete with epoxide binding to the Lewis acid and hydrogen-bond with anionic chain ends to impede epoxide ring opening. We report that a bifunctional aminocyclopropenium aluminum salen complex maintains excellent activity in the presence of protic functionality, exhibiting resilience against these inhibition pathways, even at high CTA concentrations. We apply reversible-deactivation chain transfer in the bifunctional ROCOP system to demonstrate precise molecular-weight control, CTA functional group scope, and accessible polymer architectures.

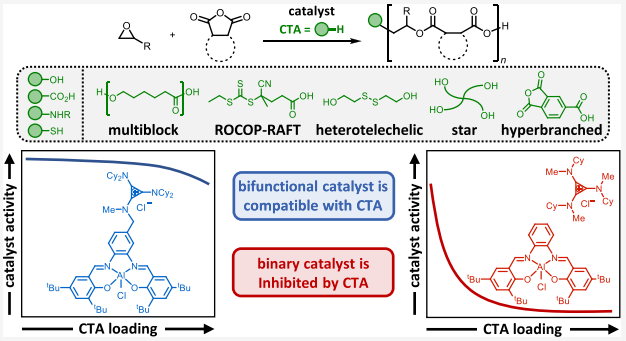


## INTRODUCTION

Ring-opening polymerizations are controlled alternatives to cumbersome polycondensation routes to synthesize aliphatic and semiaromatic polyesters.[1−6] In contrast to step-growth methods, living ring-opening polymerizations enable tunable molecular weights and low dispersities ($Đ \leq 1.3$). While ring-opening polymerizations of lactones or lactide have received significant attention, challenging monomer derivatization constrains accessible functionality and limits the range of resultant polymer properties.[7−9] By contrast, the alternating ring-opening copolymerization (ROCOP) of epoxides and cyclic anhydrides enchains a wide variety of commercially available and readily synthesized comonomer pairs with excellent control over the molecular weight and dispersity.[10,11] Living epoxide/cyclic anhydride ROCOPs are commonly catalyzed by metal salen complexes paired with nucleophilic cocatalysts; these species initiate polymerization and modulate the activity of the growing chain ends (Scheme 1a).[12−27] Adjusting the catalyst/cocatalyst/comonomer stoichiometry provides control over polymer molecular weight, but this approach produces only two polymer chains per catalyst. It is highly desirable to improve catalytic efficiency by producing multiple polymer chains per catalyst. Decreasing the catalyst loading will reduce costs, minimize toxic organometallic residue, and prevent premature polymer degradation.

Chain transfer agents (CTAs) are often employed in ring-opening copolymerizations to increase the number of polymer chains per catalyst.[28,29] In ROCOP, each equivalent of protic chain transfer agent produces a dormant chain in addition to the active anionic chains initially derived from the catalyst and cocatalyst. Polymer molecular weights therefore depend on the total initiator concentration and can be tailored by varying both the catalyst and CTA loadings. Rapid, reversible proton transfer between dormant and active chains relative to the rate of propagation (Scheme 2) ensures uniform chain growth, affording narrow molecular-weight distributions.[28] A 2011 report from our group demonstrated that the addition of isopropyl alcohol to chromium salcy-catalyzed (salcy = *N*,*N*′-bis(salicylidene)-1,2-diaminocyclohexane) copolymerizations of epoxides and maleic anhydride decreased molecular weights and dispersities in proportion to the amount of alcohol added.[14] In addition to alcohols, carboxylic acids and amines have been reported as CTAs for reversible-deactivation chain transfer in epoxide/cyclic anhydride ring-opening copolymerization (RD-ROCOP).[30,31] Recent applications of RD-

**Received:** September 18, 2020
**Published:** November 12, 2020

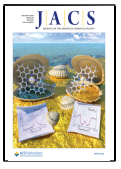

**Scheme 1. (a) Binary and (b) Bifunctional Complexes Catalyze the Alternating Ring-Opening Copolymerization of Epoxides and Cyclic Anhydrides in Conjunction with Protic Chain Transfer Agents**

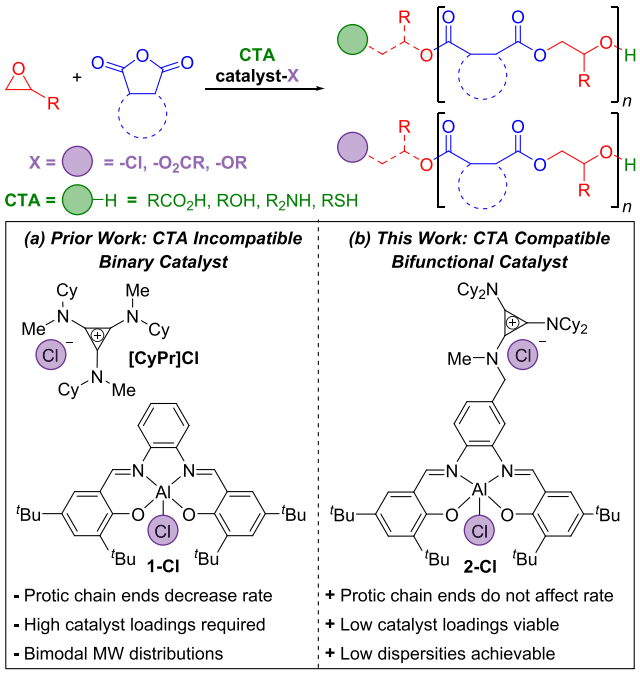


**Scheme 2. Reversible-Deactivation Chain Transfer in the Anionic Ring-Opening Copolymerization of Epoxides and Cyclic Anhydrides**

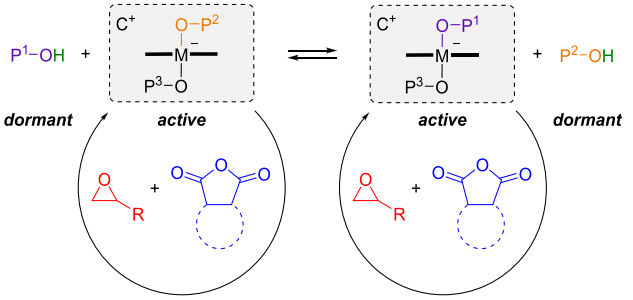


ROCOP have used multifunctional CTAs to control polyester dispersity and access both linear and star architectures.[30−32]

Binary systems comprising distinct Lewis acid complexes and nucleophilic cocatalysts have dominated epoxide/cyclic anhydride copolymerization catalysis. Yet these binary systems are vulnerable to dilution effects that retard polymerization rates at low catalyst loadings.[33] Moreover, close examination of our group's 2018 report on RD-ROCOP reveals that the addition of CTA further diminished binary aluminum salph (salph = *N*,*N*′-bis(salicylidene)phenylenediamine) catalyst activity (turnover frequency, TOF = 75 $h^{-1}$ with CTA versus 99 $h^{-1}$ without CTA).[31] Bifunctional catalysts in which the Lewis acid and cocatalyst are covalently tethered have demonstrated improved protic CTA tolerance in epoxide/$CO_2$ copolymerizations.[34,35] Although such catalysts have only sparingly been applied to epoxide/cyclic anhydride ROCOP, two terpolymerization reports suggest bifunctional catalyst compatibility with CTAs may extend to systems incorporating cyclic anhydrides.[34,36] In a series of control reactions, Lee and co-workers used a quaternary ammonium-functionalized cobalt salcy complex to polymerize propylene oxide (PO) and phthalic anhydride (PA) in the presence of ethanol CTA without notable deceleration.[34] Taken together, these reports suggest disparate rate effects of reversible-deactivation chain transfer on binary- and bifunctional-catalyzed ROCOP.

We therefore wanted to explore the differences in RD-ROCOP activity across comparable binary and bifunctional systems. We recently reported a bifunctional aluminum salph catalyst (**2-Cl**, Scheme 1b) that operates via an analogous mechanism to binary **1-Cl** in epoxide/cyclic anhydride copolymerization.[33,36] The study demonstrated that covalently tethering the Lewis acid and aminocyclopropenium cocatalyst prevents common transesterification and epimerization side reactions while maintaining high polymerization rates at low loadings. The notable differences in activities and selectivities of the binary and bifunctional systems motivated the current study aimed at understanding the effect of protic chain transfer agents on catalyst performance.

Polymerization rates slowed dramatically using binary system **1-Cl**/[CyPr]Cl ([CyPr] = tris(cyclohexylmethyl) aminocyclopropenium) and even small quantities of protic CTA (<10 equiv). Gratifyingly, **2-Cl** maintained good TOFs (>70 $h^{-1}$), even at high CTA loadings (≤50 equiv). Taking inspiration from enzymatic kinetic analysis, we demonstrate that protic chain ends can inhibit both epoxide activation at the Lewis acid and rate-limiting epoxide ring opening. Catalyst **2-Cl** minimizes these disruptions to maintain high polymerization rates in the presence of CTA, further underscoring the advantages of using a bifunctional ROCOP catalyst. Applying **2-Cl** in RD-ROCOP achieves precise molecular-weight control, expanded protic CTA scope, and direct access to advanced polymer architectures.

## RESULTS AND DISCUSSION

**Catalyst Activity in RD-ROCOP.** To elucidate the effects of protic CTA on the binary **1-Cl** and bifunctional **2-Cl** catalysts, we compared copolymerizations of PO and carbic anhydride (CPMA) at varied loadings of 1-adamantanecarboxylic acid (**3a**) (Figure 1). In the bifunctional system, polymerization rates were invariant with CTA loading up to 25 equiv of **3a** relative to 1 equiv of **2-Cl**. At higher CTA loadings (50 equiv of **3a**), rates declined only modestly and **2-Cl** maintained good activity (TOF 70 $h^{-1}$). By contrast, rates declined rapidly with increasing equivalents of **3a** in polymerizations catalyzed by **1-Cl**/[CyPr]Cl. Polymerizations performed with **1-Cl** and the more common [PPN]Cl cocatalyst exhibited nearly identical behaviors, indicating that deceleration in binary RD-ROCOP systems is not unique to the [CyPr]Cl cocatalyst (Figure 1, Table S1).

**Characterization of Active and Dormant Chain Ends.** Active and dormant chains differ only by a protonated chain end; we therefore characterized their $\omega$-termini to understand how these species impact binary- and bifunctional-catalyzed RD-ROCOP. Because of the polymerization's alternating nature, the $\omega$-terminus of any active (dormant) chain may be either an alkoxide (alcohol) or a carboxylate (carboxylic acid). On the basis of the different p$K_a$ values of the possible end groups, we hypothesized that reversible-deactivation chain transfer protonates the most basic species; that is, most dormant chains would possess alcohol end groups rather than more acidic carboxylic acid end groups.

We prepared salph aluminum complexes designed to model active alkoxide or carboxylate chain ends bound to **1**. Model


https://dx.doi.org/10.1021/jacs.0c10014
J. Am. Chem. Soc. 2020, 142, 20161−20169

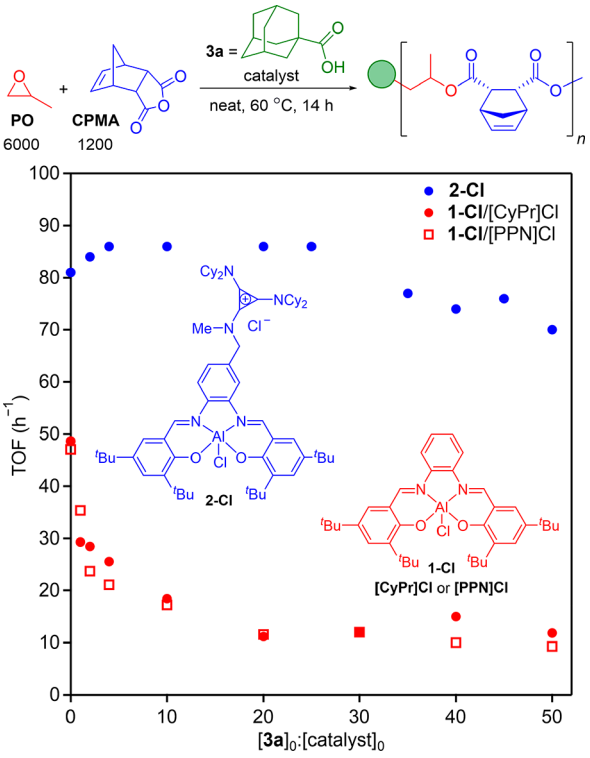


**Figure 1.** Turnover frequency as a function of **3a** concentration in binary (**1-Cl**/[CyPr]Cl) and bifunctional (**2-Cl**) catalyst systems. $[catalyst]_0$:$[CPMA]_0$:$[PO]_0$ = 1:1200:6000. For polymerizations performed using **1-Cl**, $[catalyst]_0$:$[cocatalyst]_0$ = 1:1. TOF = Turnover frequency, mol anhydride consumed × mol catalyst$^{-1}$ × h$^{-1}$.

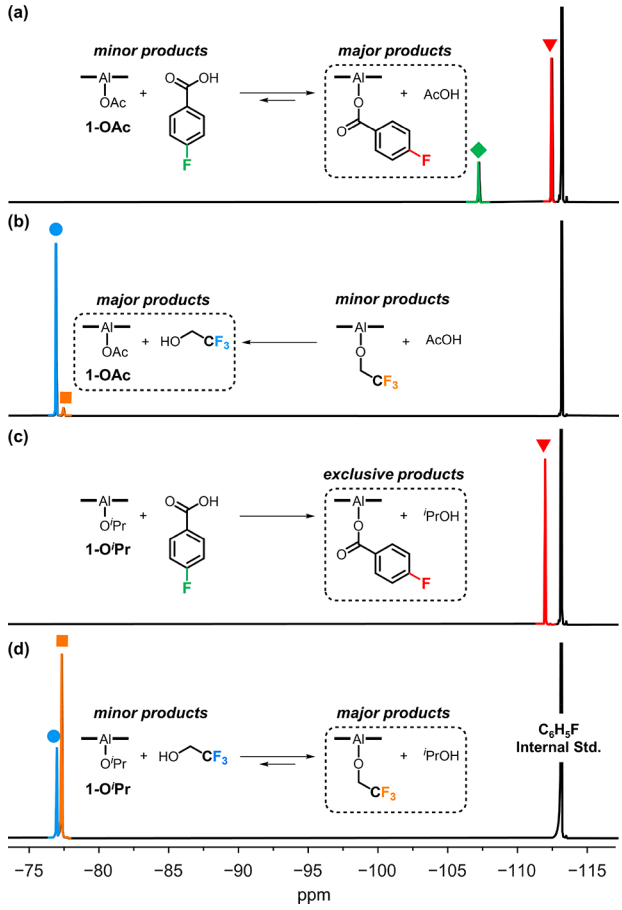


**Figure 2.** $^{19}$F NMR spectra of reactions of model complexes **1-OAc** (a and b) and **1-O$^i$Pr** (c and d) with fluorinated alcohols and carboxylic acids in THF. Referenced to fluorobenzene internal standard (−113.15 ppm, black).

salph aluminum isopropoxide (**1-O$^i$Pr**) and salph aluminum acetate (**1-OAc**) species were then each treated with either 2,2,2-trifluoroethanol or 4-fluorobenzoic acid to mimic the possible end groups of dormant chains. The equilibrium product distribution was monitored by $^{19}$F NMR in tetrahydrofuran solvent (Figure 2). Reacting either **1-O$^i$Pr** or **1-OAc** with the more acidic 4-fluorobenzoic acid produced the salph aluminum 4-fluorobenzoate complex as the major product (Figure 2a,c). Treating **1-O$^i$Pr** with 2,2,2-trifluoroethanol produced a mixture of the two salph aluminum alkoxides (Figure 2d), while reacting **1-OAc** with 2,2,2-trifluoroethanol afforded almost no conversion (Figure 2b). These studies corroborate that p$K_a$ governs reversible-deactivation chain transfer between anionic and protic chain ends.

Previous mechanistic studies performed in the absence of CTA have identified a resting state in which two propagating carboxylates bind to the Lewis acid.[6,33] MALDI-TOF analysis of PO/CPMA copolymerizations catalyzed by **2-Cl** further validate this bis-carboxylate resting state in the absence of CTA: the spectrum reveals primarily carboxylic acid end groups (Figure 3a and Figure S20). For copolymerizations performed using CTA **3a** and **2-Cl**, the MALDI-TOF spectrum reveals mass distributions dominated by alcohol end groups (Figure 3b and Figure S19). This prevalence of alcohol chain ends in RD-ROCOP is consistent with the small-molecule $^{19}$F NMR equilibrium studies: given the two possible protic chain end resting states, the higher p$K_a$ alcohol predominates.

**RD-ROCOP Mechanism.** We investigated the kinetic behavior of RD-ROCOP to understand how alcohol chain ends interact with the binary and bifunctional catalysts. Examining the reaction profiles of PO/CPMA copolymerizations catalyzed by either **1-Cl**/[CyPr]Cl or **2-Cl** reveals no evidence of an induction period caused by CTA (Figures S30 and S38). We therefore conclude the rate retardation in the presence of alcohol chain ends arises from a change in mechanism or persistent inhibition throughout the polymerization.

Epoxide/cyclic anhydride ROCOP can proceed via two possible catalytic cycles sharing a common alkoxide/carboxylate intermediate; this mixed alkoxide/carboxylate complex may ring-open either epoxide or cyclic anhydride. In the absence of CTA, cyclic anhydride is ring-opened more rapidly than epoxide such that the primary propagation cycle proceeds via carboxylate/carboxylate and carboxylate/alkoxide intermediates.[6] Performing a competition experiment in the presence of *tert*-butanol (**3c**) revealed that the mixed alkoxide/carboxylate species first ring-opens 1 equiv of CPMA, after which CPMA and PO are consumed at similar rates (Figure S33). Accordingly, the presence of protic species does not change the primary propagation cycle. Variable time normalization analysis was used to identify reaction orders in the comonomers and catalytic components.[37,38] In RD-ROCOP using CTA **3a** and either binary or bifunctional catalyst, reaction rates exhibited a zero-order dependence on cyclic anhydride, a first-order dependence on epoxide, and a first-order dependence on each catalytic unit (**1-Cl** and


https://dx.doi.org/10.1021/jacs.0c10014
J. Am. Chem. Soc. 2020, 142, 20161−20169

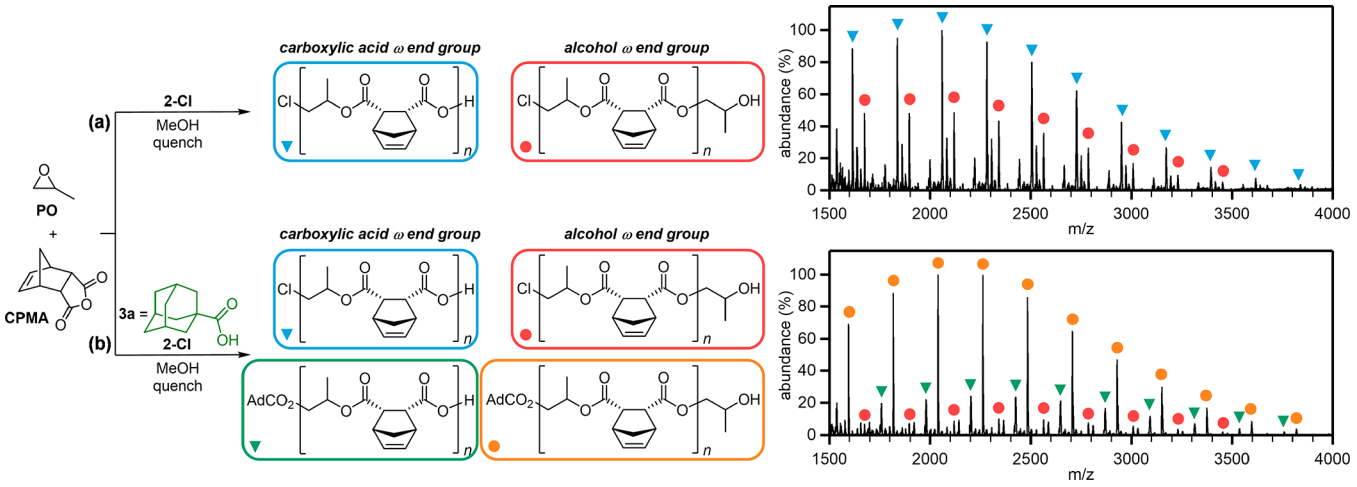


**Figure 3.** MALDI-TOF spectra of PO/CPMA copolymers synthesized in the absence (a) and presence (b) of CTA **3a**, demonstrating that alcohol chain ends predominate in RD-ROCOP. In (a), $[\mathbf{2\text{-}Cl}]_0$:$[CPMA]_0$:$[PO]_0$ = 1:50:250, and in (b), $[\mathbf{2\text{-}Cl}]_0$:$[\mathbf{3a}]_0$:$[CPMA]_0$:$[PO]_0$ = 1:10:300:1500. Reactions were quenched with methane sulfonic acid in methanol prior to full conversion of cyclic anhydride (~55%) to obtain polymers comprising representative end-group distributions. Control experiments validate that alcohol- and carboxylic acid-terminated chains ionize with similar efficiencies (Table S8, Figures S23–S25). See the Supporting Information for assignment of minor components (Figures S21 and S22).

[CyPr]Cl or **2-Cl**) (Figures S34–S41). These reaction orders are consistent with pre-equilibrium epoxide binding and rate-limiting epoxide ring opening, as observed in ROCOP systems in the absence of CTA.[6,33]

While the primary enchainment mechanism is unchanged by the presence of alcohol chain ends, two discrepancies in kinetic behavior suggest possible inhibition pathways. In the absence of CTA, saturation kinetic behavior in epoxide was observed at high PO concentrations ($[PO]_0 \geq 10$ M, $[CPMA]_0$:$[PO]_0$ = 1:5).[6,33] Intriguingly, reversible-deactivation copolymerizations using **3a** and **1-Cl**/[CyPr]Cl remained first-order in PO, even when performed neat ($[CPMA]_0$:$[PO]_0$ = 1:5, Figure S36). Second, in RD-ROCOP catalyzed by **2-Cl**, exogenous [CyPr]Cl cocatalyst did not accelerate rate-limiting ring opening until the concentration of anionic chain ends exceeded that of protic chain ends ($[CyPrCl]_0 + 2 \times [\mathbf{2\text{-}Cl}]_0 > [\mathbf{3a}]_0$) (Table S9). We therefore propose two possible mechanisms by which alcohol chain ends may inhibit RD-ROCOP (Scheme 3). First, the Lewis basic alcohol $\omega$-terminus of dormant chains may compete with epoxide to bind the Lewis acid catalyst. Alternatively, hydrogen-bond donation by alcohol chain ends may attenuate the nucleophilicity of the growing anionic chain. These hypotheses prompted further kinetic investigation into the mechanism of inhibition in RD-ROCOP.

**Lineweaver–Burk Analysis of Inhibition in RD-ROCOP.** The observed Michaelis–Menten kinetic behavior in RD-ROCOP (*vide supra*) permits enzymatic inhibition analysis. Lineweaver–Burk plots of inverse initial rate versus inverse PO concentration were constructed at various inhibitor concentrations ($[P_n\text{–OH}] = [\mathbf{3a}]_0$ after initiation) to graphically distinguish inhibition pathways (Figure 4).[39] Best fit lines that have a common intersection on the *y*-axis indicate that the theoretical maximum polymerization rate is invariant with $[P_n\text{–OH}]$, but higher PO concentrations are required to achieve it. In this case, alcohol chain ends compete with epoxide to bind the Lewis acid but do not affect monomer enchainment. Conversely, best fit lines that share a common intersection on the *x*-axis suggest the theoretical maximum copolymerization rate depends on $[P_n\text{–OH}]$ rather than $[PO]_0$. Such noncompetitive inhibition is consistent with hydrogen bonding between alcohol and anionic chain ends slowing epoxide ring opening. An off-axis common intersection point suggests both competitive binding and hydrogen-bonding inhibition pathways contribute to decelerated polymerization rates.

**Scheme 3. Proposed Polymerization Mechanism and Inhibition Pathways of ROCOP in the Presence of CTA**[a]

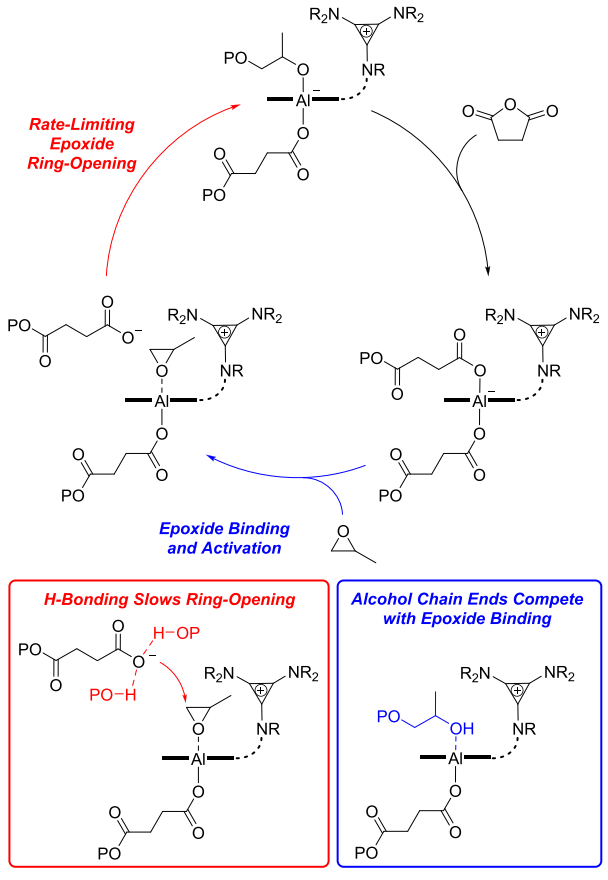


[a]Monomer, catalyst, and cocatalyst structures truncated for clarity.


https://dx.doi.org/10.1021/jacs.0c10014
J. Am. Chem. Soc. 2020, 142, 20161–20169

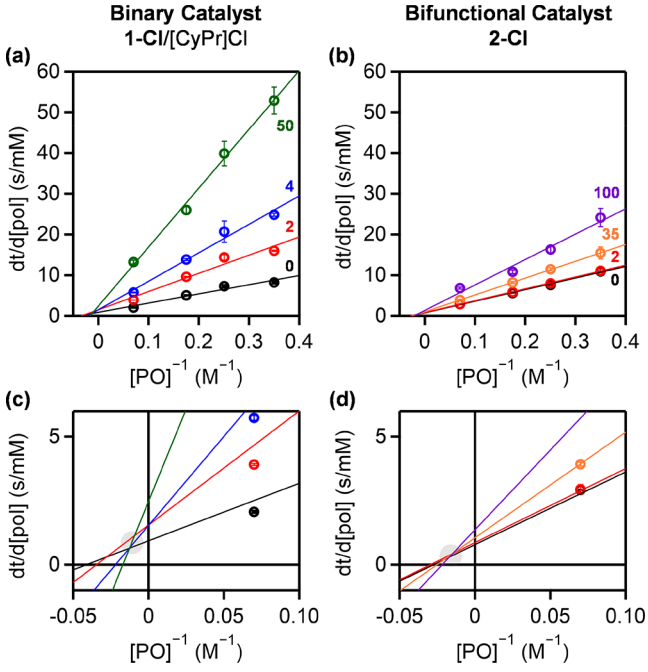


**Figure 4.** Lineweaver–Burk plots of inhibition by CTA **3a** in the binary (a and c, left) and bifunctional (b and d, right) catalyst systems. Top plots (a and b) show full kinetic analyses where each point represents the mean of four independent measurements at each PO concentration and **3a** loading (equivalents of CTA relative to the catalyst noted on plots). Bottom plots (c and d) are magnified replicates to show common intersection points (highlighted with gray circles).

Copolymerizations using **3a** and **1-Cl**/[CyPr]Cl exhibit mixed inhibition with best fit lines exhibiting a common intersection in the second quadrant (−,+) (Figure 4a,c): Alcohol chain ends therefore both compete with epoxide to bind the Lewis acid and hydrogen-bond to anionic chains to slow ring opening. As high CTA loadings do not fully suppress reversible-deactivation ROCOP, ring opening by H-bonded chains is slow but productive. By contrast, Lineweaver–Burk analysis of **2-Cl**-catalyzed RD-ROCOP reveals a common intersection nearer to the *x*-axis (Figure 4b,d), consistent with a predominantly noncompetitive inhibition pathway. We recently reported that **2-Cl** prevents transesterification and epimerization side reactions by keeping anionic chain ends associated with the Lewis acid.[33] We propose that covalently tethering the aluminum salph and aminocyclopropenium cocatalyst in **2-Cl** favors the hexacoordinate aluminate complex, suppressing competitive binding of alcohol chain ends at the Lewis acid. Moreover, bifunctional **2-Cl** appears only modestly affected by hydrogen bonding between anionic and alcohol chain ends; intramolecular epoxide ring opening within the catalytic unit may exclude dormant chains to mitigate this effect.

**Monomer Scope.** We sought to further validate that the rate effects observed using **1-Cl** and **2-Cl** in RD-ROCOP are a feature of catalysis, rather than the PO/CPMA comonomers. To this end, we applied **1-Cl**/[CyPr]Cl or **2-Cl** in copolymerizations of other epoxides and cyclic anhydrides with and without CTA **3a** (Tables S5 and S6). Copolymerizations of CPMA with epoxides bearing larger substituents (*tert*-butyl glycidyl ether, $^t$BGE, or 1,2-epoxy-5-hexene, EHX) catalyzed by **2-Cl** exhibited somewhat slower rates as compared to those incorporating PO (TOF = 22 or 52 $h^{-1}$ versus 86 $h^{-1}$, respectively). Nonetheless, the addition of 10 equiv of **3a** did not affect the activity of **2-Cl** (TOF = 24 $h^{-1}$ for $^t$BGE, 54 $h^{-1}$ for EHX). By contrast, the activity of **1-Cl**/[CyPr]Cl was nearly halved by the addition of 10 equiv of **3a** in copolymerizations of CPMA with $^t$BGE (TOF = 7 and 3.5 $h^{-1}$) or EHX (TOF = 13 and 7 $h^{-1}$). Copolymerizations of PO and PA exhibited similar behavior: the addition of **3a** did not affect the activity of **2-Cl** (TOF = 114 and 117 $h^{-1}$) but did decrease the efficacy of **1-Cl**/[CyPr]Cl (TOF = 95 and 56 $h^{-1}$). Interestingly, the addition of **3a** to copolymerizations of PO and 4-chlorophthalic anhydride (Cl-PA) did not significantly affect the activity of either **2-Cl** (TOF = 82 and 81 $h^{-1}$) or **1-Cl**/[CyPr]Cl (TOF = 48 and 42 $h^{-1}$). These results confirm that **2-Cl** maintains good activity in RD-ROCOP of a variety of epoxide and cyclic anhydride comonomers.

**Molecular-Weight Control in RD-ROCOP.** A key advantage of RD-ROCOP is the ability to control molecular weight at reduced catalyst loadings: Molecular weight depends on the total concentration of catalyst and CTA and may therefore be controlled independently of $[\mathbf{2\text{-}Cl}]_0$. As expected, increasing equivalents of CTA **3a** relative to those of **2-Cl** resulted in decreasing molecular weight (Figure 5a, Table S2,

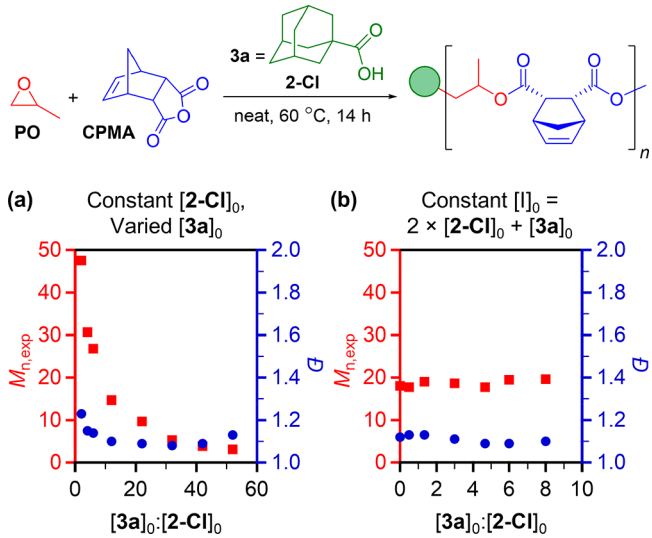


**Figure 5.** Effect of CTA **3a** concentration on PO/CPMA copolymerization using bifunctional catalyst **2-Cl**. (a) Increasing $[\mathbf{3a}]_0$ relative to fixed $[\mathbf{2\text{-}Cl}]_0$ ($[\mathbf{2\text{-}Cl}]_0$:$[CPMA]_0$:$[PO]_0$ = 1:1200:6000, $[\mathbf{3a}]_0$ = 0–50). (b) Holding total initiating species constant while varying $[\mathbf{3a}]_0/[\mathbf{2\text{-}Cl}]_0$ ($[I]_0 = 2 \times [\mathbf{2\text{-}Cl}]_0 + [\mathbf{3a}]_0 = 10$, $[CPMA]_0$:$[PO]_0$ = 1200:6000).

entries 1–8). RD-ROCOP can also be used to reduce the catalyst loading required to achieve a targeted molecular weight by maintaining a constant concentration of total initiating species ($2 \times [\mathbf{2\text{-}Cl}]_0 + [\mathbf{3a}]_0$), Figure 5b, Table S2, entries 9–15. Decreasing $[\mathbf{2\text{-}Cl}]_0$ while proportionately increasing $[\mathbf{3a}]_0$ afforded polyesters with molecular weights in the narrow range of ∼18–19 kDa while maintaining low dispersities. Notably, decreasing $[\mathbf{2\text{-}Cl}]_0$ in the presence of CTA had no measurable influence on catalyst activity at each loading (TOF = 86–89 $h^{-1}$). These results demonstrate the remarkable advantages of using bifunctional **2-Cl** in RD-


https://dx.doi.org/10.1021/jacs.0c10014
J. Am. Chem. Soc. 2020, 142, 20161–20169

ROCOP to simultaneously control polymer molecular weight and reduce catalyst loadings without loss of catalytic activity.

**CTA Functional Group Scope.** We next examined other protic functional groups as viable CTAs (**3a**–**3m**) for RD-ROCOP of PO and CPMA (Table 1). Successful chain transfer by each functional group was assessed by comparing $M_{n,GPC}$ to the molecular weight calculated on complete initiation by **3** and **2-Cl** ($M_{n,th}$). Excellent agreement between $M_{n,GPC}$ and $M_{n,th}$ was observed for polymerizations employing CTAs possessing carboxylic acid (**3a**), unhindered alcohol (**3b** and **3e**), amine (**3g**, **3h**, and **3j**), and thiol (**3k**) functional groups. Meanwhile, sterically hindered (**3c** and **3d**) or weakly nucleophilic (**3l** and **3m**) functional groups performed poorly as CTAs with noticeable discrepancies in $M_{n,GPC}$ and $M_{n,th}$ values and increased dispersities. Polymerizations employing sterically hindered **3c** gave intermediate $M_{n,GPC}$ values with a low-molecular-weight tail (Figure S3), consistent with partial chain transfer. Polymerizations using **3d** demonstrated that increasing the steric bulk surrounding the alcohol unit fully suppressed chain transfer. Polymerizations performed using **3f** or **3i** gave $M_{n,GPC}$ values in agreement with values expected for initiation only by **2-Cl**, indicating chain transfer did not occur. Despite the structural similarity of naphthylamines **3i** and **3j**, only polymerizations employing primary naphthylamine **3j** gave $M_{n,GPC}$ values consistent with the $M_{n,th}$ expected for chain transfer. Attenuated polymerization rates were also observed when using CTAs *N*-methylbenzamide (**3f**, TOF = 76 $h^{-1}$) and dimethylurea (**3l**, TOF = 50 $h^{-1}$), which suggests that highly polar protic functional groups such as amides and ureas can inhibit ROCOP when using bifunctional catalysts.

**Table 1. Protic Functional Groups Screened as Chain Transfer Agents for PO/CPMA Copolymerization**[a]

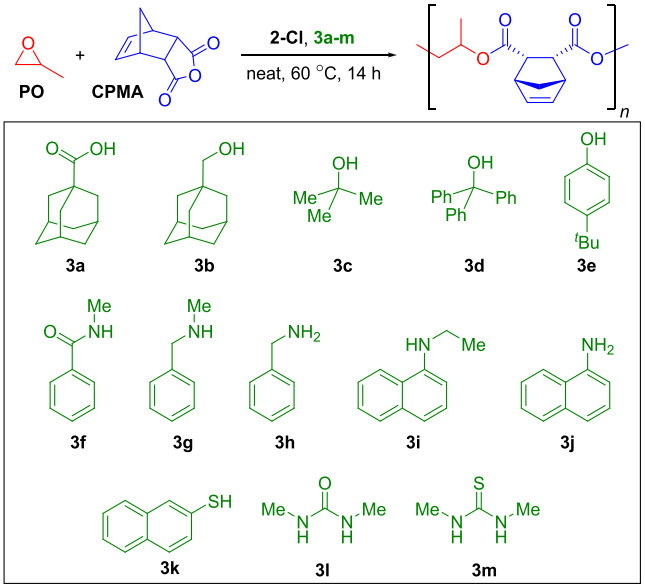


| entry | CTA | conv[b] (%) | TOF[c] ($h^{-1}$) | $M_{n,th}$[d] (kDa) | $M_{n,GPC}$[e] (kDa) | $Đ$[e] |
|---|---|---|---|---|---|---|
| 1[f] | | 94 | 81 | 125.3 | 47.5 | 1.23 |
| 2 | **3a** | >99 | 86 | 22.2 | 14.7 | 1.10 |
| 3 | **3b** | >99 | 86 | 22.2 | 14.6 | 1.11 |
| 4 | **3c** | >99 | 86 | 22.2 | 29.5 | 1.28 |
| 5 | **3d** | 96 | 82 | 21.3 | 45.1 | 1.26 |
| 6 | **3e** | >99 | 86 | 22.2 | 15.7 | 1.09 |
| 7 | **3f** | 88 | 76 | 19.6 | 39.1 | 1.25 |
| 8 | **3g** | >99 | 86 | 22.2 | 18.4 | 1.09 |
| 9[g] | **3h** | 74 | 63 | 16.4 | 14.0 | 1.14 |
| 10[h] | **3h** | 18 | 15 | 4.1 | 2.4 | 1.33 |
| 11 | **3i** | 96 | 82 | 21.3 | 49.2 | 1.18 |
| 12[g] | **3j** | >99 | 86 | 22.2 | 17.3 | 1.11 |
| 13[h] | **3j** | 38 | 33 | 8.6 | 6.3 | 1.12 |
| 14 | **3k** | >99 | 86 | 22.2 | 16.1 | 1.09 |
| 15 | **3l** | 58 | 50 | 12.9 | 15.6 | 1.34 |
| 16 | **3m** | >99 | 86 | 22.2 | 20.9 | 1.10 |

[a] [**2-Cl**]$_0$:[**3**]$_0$:[CPMA]$_0$:[PO]$_0$ = 1:10:1200:6000. [b] Determined by $^1$H NMR analysis of the crude reaction mixture. [c] TOF = Turnover frequency, mol of anhydride consumed × mol of **2-Cl**$^{-1}$ × $h^{-1}$. [d] $M_{n,th}$ calculated assuming complete initiation by **3**. [e] Determined by GPC in THF, calibrated with polystyrene standards. [f] No CTA was used, [**2-Cl**]$_0$:[CPMA]$_0$:[PO]$_0$ = 1:1200:6000. [g] **3** added prior to PO. [h] **3** added after PO.

To further corroborate the chain transfer results summarized in Table 1, we prepared low-molecular-weight polymers using **2-Cl** and **3a**–**3m** for end group analysis by MALDI-TOF mass spectrometry (Table S3, Figures S5–S17). Polymerizations performed using CTAs **3a**, **3b**, **3e**, **3g**, **3h**, **3j**, and **3k** afforded low-molecular-weight polymers that were subsequently analyzed by MALDI-TOF mass spectrometry. Polymers synthesized using **3c**, **3d**, **3f**, **3i**, **3l**, and **3m** possessed molecular weights that exceeded the detection limit of the instrument used for MALDI-TOF analysis, corroborating that these species do not promote chain transfer.

Interestingly, only water-derived chains were observed by MALDI-TOF analysis when primary amine CTAs **3h** (Figure S11) or **3j** (Figure S9) were combined with **2-Cl** and CPMA prior to the addition of PO (Table 1, entries 9 and 12). We hypothesized that the reaction of **3h** and **3j** with CPMA formed the corresponding imides and 1 equiv of water, which then functioned as the CTA to give water-derived chains. To test this hypothesis, we combined **3j**, CPMA, and **2-Cl** in THF and heated at 60 °C for 4 h. $^1$H NMR analysis of the crude reaction mixture revealed primary formation of the imide derived from **3j** and CPMA (Figure S18). These results corroborate the MALDI-TOF data that primary amines do not function directly as CTAs when added to the polymerization prior to PO. Instead, most chains are initiated by the water produced as a byproduct of imide formation. To study the effect of the catalyst on imide formation, we combined **3j** and CPMA in THF at 60 °C for 4 h in the absence of **2-Cl**. $^1$H NMR analysis of the crude reaction mixture revealed primarily the amide-acid intermediate formed from ring opening of CPMA by **3j** (Figure S19). This result corroborates that **2-Cl** catalyzes ring closing of the amide-acid to the corresponding imide with concomitant formation of water.

To assess whether primary amines might function as CTAs if imide formation were suppressed, we investigated the effect of the CTA order of addition. **2-Cl**, CPMA, and PO were first combined, followed by the addition of **3h** or **3j** prior to heating at 60 °C. In contrast to the water-derived chains obtained when **3h** or **3j** were added before PO, MALDI-TOF analysis revealed that adding **3h** or **3j** as the last reagent produced polymer chains that were primarily initiated by **3h** (Figure S10) or **3j** (Figure S12) with a secondary distribution of chloride-initiated chains derived from **2-Cl**. We reason that prior to the addition of the primary amine, **2-Cl**, CPMA, and PO rapidly react to give the corresponding coordinatively saturated complex **2-X$_2$** (Scheme 4a). A detailed mechanistic


https://dx.doi.org/10.1021/jacs.0c10014
J. Am. Chem. Soc. 2020, 142, 20161–20169

**Scheme 4. Effect of Primary Amine CTA Order of Addition on Imide Formation and Chain Transfer during RD-ROCOP**

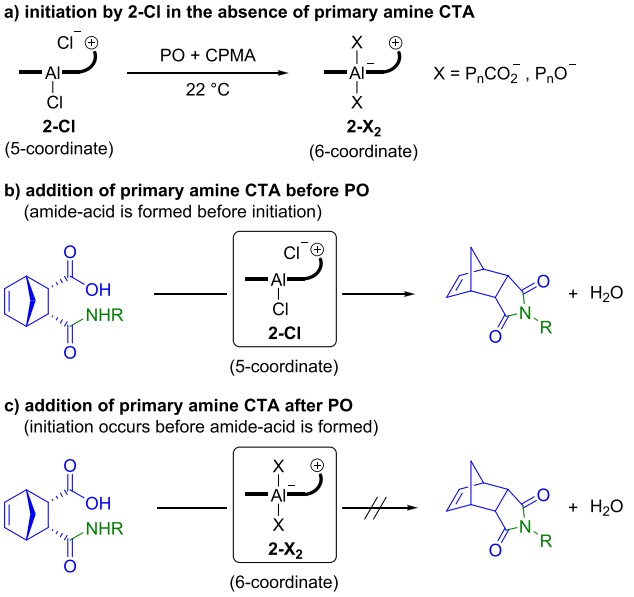


study by Fieser *et al.* showed that initiation with the analogous **1-Cl**/[PPN]Cl binary catalyst system is rapid, leading to the formation of a bis-alkoxide complex that can react further with cyclic anhydride.[6] Given that an open coordination site is likely required for amide-acid ring closure (Scheme 4b), we hypothesize that the formation of coordinatively saturated **2-$X_2$** prior to the amide-acid prevents Lewis acid catalyzed imide formation, allowing the amide-acid to initiate polymerization (Scheme 4c).

**Advanced Polymer Architectures via RD-ROCOP.** We next applied the high activity and functional group tolerance of **2-Cl** in RD-ROCOP to prepare polyester-based architectures that would otherwise be inaccessible using binary catalyst systems. To demonstrate the versatility of bifunctional catalyst **2-Cl**, we synthesized telechelic, multiblock, and branched polyesters by RD-ROCOP using multifunctional CTAs **3n**−**3u** (Table 2). Dihydroxy-functional CTAs (**3n** and **3o**) afforded difunctional polyesters. To access heterotelechelic materials, we reduced the disulfide-containing polyester derived from CTA **3o** with excess dithiothreitol (DTT). The molecular weight of the polyester following reduction ($M_{n,GPC}$ = 2.5) was approximately half that of the parent polymer ($M_{n,GPC}$ = 5.7), as evidenced by a complete shift in the GPC RI peak of the parent polymer to a higher elution volume (Figure S20b, Table S4). Cleavage of the central disulfide linkage may enable orthogonal postpolymerization modification of the hydroxy-thiol polymer chain ends.

MacroCTAs (**3p** and **3q**) underwent efficient chain transfer to give the corresponding ABA triblock copolymers with low dispersities ($Đ$ < 1.20). Of note, chain extension of poly(ε-caprolactone) (**3q**) occurred without transesterification to the sterically unhindered polyester backbone. As discussed in prior work, **2-Cl** is particularly adept at preventing such side reactions.[33]

Tetrafunctional CTA **3r** was successfully chain-extended to the corresponding star copolymer with poly(ethylene oxide) core and polyester outer block. Uniform polymer growth from each arm was evidenced by the near monomodal GPC trace

**Table 2. Protic Chain Transfer Agents for PO/CPMA Copolymerization Affording Various Polymer Architectures[a]**

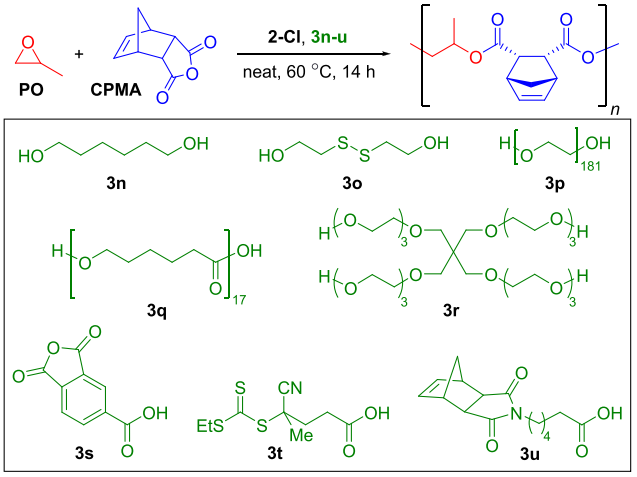


| entry | CTA | conv[b] (%) | TOF[c] ($h^{-1}$) | $M_{n,GPC}$[d] (kDa) | $Đ$[d] |
|---|---|---|---|---|---|
| 1 | **3n** | >99 | 86 | 15.3 | 1.08 |
| 2 | **3o** | >99 | 86 | 15.2 | 1.10 |
| 3 | **3p** | >99 | 86 | 34.3 | 1.17 |
| 4 | **3q** | 96 | 82 | 13.3 | 1.16 |
| 5 | **3r** | >99 | 86 | 19.6 | 1.10 |
| 6[e] | **3s** | 79 | 43 | 12.0 | 1.79 |
| 7 | **3t** | >99 | 86 | 15.7 | 1.14 |
| 8 | **3u** | >99 | 86 | 13.5 | 1.08 |

[a][**2-Cl**]$_0$:[**3**]$_0$:[CPMA]$_0$/[PO]$_0$ = 1:10:1200:6000. [b]Determined by $^1$H NMR analysis of the crude reaction mixture. [c]TOF = Turnover frequency, mol of anhydride consumed × mol of **2-Cl**$^{-1}$ × $h^{-1}$. [d]Determined by GPC in THF, calibrated with polystyrene standards. [e][**2-Cl**]$_0$:[**3s**]$_0$:[CPMA]$_0$/[PO]$_0$ = 1:50:1150:6000, 22 h.

and low dispersity ($Đ$ = 1.19) of the star copolymer. 1,3,4-Benzene tricarboxylic anhydride (**3s**) was employed as a polymerizable CTA to produce a hyperbranched polyester with a high dispersity ($Đ$ = 1.79) and broad GPC trace (Figure S4), which is likely a consequence of nonuniform branching. Furthermore, catalyst activity was reduced when using **3s** (TOF = 43 $h^{-1}$) as compared to the other CTAs summarized in Table 2 (TOFs = 84−86 $h^{-1}$), which may be due in part to the high CTA loading (50 equiv). Steric hindrance impeding efficient chain transfer likely further contributes to the suppressed reaction rate and high dispersity observed using CTA **3s**.

Recently, Wang and co-workers demonstrated simultaneous ROCOP and reversible addition-fragmentation chain transfer (RAFT) polymerization using a bifunctional CTA comprising carboxylic acid and trithiocarbonate groups.[40] Similarly, we employed trithiocarbonate-containing bifunctional CTA **3s** to synthesize a diblock copolymer using sequential RD-ROCOP and RAFT polymerization. **3s** was chain-extended with PO and PA to give macroRAFT agent **P1** ($M_{n,GPC}$ = 3.6 kDa, $Đ$ = 1.08). **P1** was then chain-extended with ethyl acrylate by RAFT polymerization to give polyester-*b*-poly(ethyl acrylate) **P2** ($M_{n,GPC}$ = 37.1 kDa, $Đ$ = 1.25) (Figure S20a, Table S4).

## CONCLUSION

Replacing catalyst equivalents with chain transfer agent can significantly improve catalytic efficiency in epoxide/cyclic anhydride copolymerizations while minimizing catalyst residue.


https://dx.doi.org/10.1021/jacs.0c10014
J. Am. Chem. Soc. 2020, 142, 20161−20169

Yet modest amounts of CTA inhibit polymerization in the predominant binary catalyst systems **1-Cl**/[PPN]Cl and **1-Cl**/[CyPr]Cl, producing prohibitively slow polymerization rates (TOF = 10−20 $h^{-1}$ when $[\mathbf{3a}]_0$:$[\mathbf{1\text{-}Cl}]_0$ > 4:1 at $[\mathbf{1\text{-}Cl}]_0$:$[CPMA]_0$ = 1:1200). Kinetic analyses reveal that alcohol chain ends disrupt epoxide activation and slow epoxide ring opening in binary-catalyzed RD-ROCOP. By contrast, bifunctional catalyst **2-Cl** maintains good activity at high CTA loadings (TOF ≅ 85 $h^{-1}$ when $[\mathbf{3a}]_0$:$[\mathbf{2\text{-}Cl}]_0 \leq$ 25:1, TOF > 70 $h^{-1}$ when $[\mathbf{3a}]_0$:$[\mathbf{2\text{-}Cl}]_0$ = 25:1−50:1). Inhibition analysis reveals that the bifunctional system minimizes competitive inhibition and mitigates slow epoxide ring opening caused by hydrogen bonding between alcohol and anionic chain ends. Applying bifunctional **2-Cl** with a variety of protic species reveals the scope of functional groups competent for chain transfer and the diversity of accessible polymer architectures. Resilience toward chain transfer agents and protic species is an underappreciated advantage of bifunctional ROCOP catalysts.

## ■ ASSOCIATED CONTENT

### Supporting Information

The Supporting Information is available free of charge at https://pubs.acs.org/doi/10.1021/jacs.0c10014.

Synthetic procedures, characterization data of all new compounds, polymerization data, and expanded mechanistic data (PDF)

## ■ AUTHOR INFORMATION


### Corresponding Author

**Geoffrey W. Coates** − *Department of Chemistry and Chemical Biology, Baker Laboratory, Cornell University, Ithaca, New York 14853-1801, United States;* orcid.org/0000-0002-3400-2552; Email: coates@cornell.edu

### Authors

**Claire A. L. Lidston** − *Department of Chemistry and Chemical Biology, Baker Laboratory, Cornell University, Ithaca, New York 14853-1801, United States;* orcid.org/0000-0002-4541-8190

**Brooks A. Abel** − *Department of Chemistry and Chemical Biology, Baker Laboratory, Cornell University, Ithaca, New York 14853-1801, United States;* orcid.org/0000-0002-2288-1975

Complete contact information is available at: https://pubs.acs.org/10.1021/jacs.0c10014

### Author Contributions

#C.A.L.L. and B.A.A. contributed equally to this work.


### Notes

The authors declare no competing financial interest.

## ■ ACKNOWLEDGMENTS

This research was supported by the Center for Sustainable Polymers, a National Science Foundation (NSF) Center for Chemical Innovation (CHE-1413862). C.A.L.L. gratefully acknowledges a graduate fellowship from the National Science Foundation (DGE-1650441). This work made use of the CCMR Shared Experimental Facilities and the NMR Facility at Cornell University, which are supported by the NSF (DMR-1719875 and CHE-1531632, respectively).

## ■ REFERENCES


(1) Hillmyer, M. A.; Tolman, W. B. Aliphatic Polyester Block Polymers: Renewable, Degradable, and Sustainable. *Acc. Chem. Res.* **2014**, *47*, 2390−2396.

(2) Ragasuskas, A. J.; Williams, C. K.; Davison, B. H.; Britovsek, G.; Cairney, J.; Eckert, C. A.; Frederick, W. J., Jr.; Hallett, J. P.; Leak, D. J.; Liotta, C. L.; Mielenz, J. R.; Murphy, R.; Templer, R.; Tschaplinski, T. The Path Forward for Biofuels and Biomaterials. *Science* **2006**, *311*, 484−489.

(3) Gross, R. A.; Kalra, B. Biodegradable Polymers for the Environment. *Science* **2002**, *297*, 803−807.

(4) Goodman, I. Polyesters. In *Encyclopedia of Polymer Science and Engineering*; Mark, H. F., Bikales, N. M., Overberger, C. G., Menges, G., Eds.; Wiley-Interscience: New York, 1988; pp 1−75.

(5) Fakirov, S. *Handbook of Thermoplastic Polyesters*; Wiley: New York, 2002.

(6) Fieser, M. E.; Sanford, M. J.; Mitchell, L. A.; Dunbar, C. R.; Mandal, M.; Van Zee, N. J.; Urness, D. M.; Cramer, C. J.; Coates, G. W.; Tolman, W. B. Mechanistic Insights into the Alternating Copolymerization of Epoxides and Cyclic Anhydrides Using a (Salph)AlCl and Iminium Salt Catalytic System. *J. Am. Chem. Soc.* **2017**, *139*, 15222−15231.

(7) Williams, C. K. Synthesis of functionalized biodegradable polyesters. *Chem. Soc. Rev.* **2007**, *36*, 1573−1580.

(8) Cairns, S. A.; Schultheiss, A.; Shaver, M. P. A broad scope of aliphatic polyesters prepared by elimination of small molecules from sustainable 1,3-dioxolan-4-ones. *Polym. Chem.* **2017**, *8*, 2990−2996.

(9) Buchard, A.; Carbery, D. R.; Davidson, M. G.; Ivanova, P. K.; Jeffery, B. J.; Kociok-Köhn, G. I.; Lowe, J. P. Preparation of Stereoregular Isotactic Poly(mandelic acid) through Organocatalytic Ring-Opening Polymerization of a Cyclic Carboxyanhydride. *Angew. Chem., Int. Ed.* **2014**, *53*, 13858−13861.

(10) Paul, S.; Zhu, Y.; Romain, C.; Brooks, R.; Saini, P. K.; Williams, C. K. Ring-opening copolymerization (ROCOP): synthesis and properties of polyesters and polycarbonates. *Chem. Commun.* **2015**, *51*, 6459−6479.

(11) Longo, J. M.; Sanford, M. J.; Coates, G. W. Ring-Opening Copolymerization of Epoxides and Cyclic Anhydrides with Discrete Metal Complexes: Structure-Property Relationships. *Chem. Rev.* **2016**, *116*, 15167−15197.

(12) Robert, C.; deMontigny, F.; Thomas, C. M. Tandem Synthesis of Alternating Polyesters from Renewable Resources. *Nat. Commun.* **2011**, *2*, 586.

(13) Darensbourg, D. J.; Poland, R. R.; Escobedo, C. Kinetic Studies on the Alternating Copolymerization of Cyclic Acid Anhydrides and Epoxides, and the Terpolymerization of Cyclic Acid Anhydrides, Epoxides, and $CO_2$ Catalyzed by (salen)$Cr^{III}Cl$. *Macromolecules* **2012**, *45*, 2242−2248.

(14) DiCiccio, A. M.; Coates, G. W. Ring-Opening Copolymerization of Maleic Anhydride with Epoxides: A Chain-Growth Approach to Unsaturated Polyesters. *J. Am. Chem. Soc.* **2011**, *133*, 10724−10727.

(15) Longo, J. M.; DiCiccio, A. M.; Coates, G. W. Poly(propylene succinate): A New Polymer Stereocomplex. *J. Am. Chem. Soc.* **2014**, *136*, 15897−15900.

(16) Van Zee, N. J.; Coates, G. W. Alternating Copolymerization of Propylene Oxide with Biorenewable Terpene-Based Cyclic Anhydrides: A Sustainable Route to Aliphatic Polyesters with High Glass Transition Temperatures. *Angew. Chem., Int. Ed.* **2015**, *54*, 2665−2668.

(17) Sanford, M. J.; Peña Carrodeguas, L.; Van Zee, N. J.; Kleij, A. W.; Coates, G. W. Alternating Copolymerization of Propylene Oxide and Cyclohexene Oxide with Tricyclic Anhydrides: Access to Partially Renewable Aliphatic Polyesters with High Glass Transition Temperatures. *Macromolecules* **2016**, *49*, 6394−6400.

(18) DiCiccio, A. M.; Longo, J. M.; Rodriguez-Calero, G. G.; Coates, G. W. Development of Highly Active and Regioselective Catalysts for the Copolymerization of Epoxides with Cyclic Anhydrides: An

Unanticipated Effect of Electronic Variation. *J. Am. Chem. Soc.* **2016**, *138*, 7107−7113.
(19) Van Zee, N. J.; Sanford, M. J.; Coates, G. W. Electronic Effects of Aluminum Complexes in the Copolymerization of Propylene Oxide with Tricyclic Anhydrides: Access to Well-Defined Functionalizable Aliphatic Polyesters. *J. Am. Chem. Soc.* **2016**, *138*, 2755−2761.
(20) Liu, J.; Bao, Y.-Y.; Liu, Y.; Ren, W.-M.; Lu, X.-B. Binuclear Chromium-Salen Complex Catalyzed Alternating Copolymerization of Epoxides and Cyclic Anhydrides. *Polym. Chem.* **2013**, *4*, 1439−1444.
(21) Li, J.; Ren, B.-H.; Chen, S.-Y.; He, G.-H.; Liu, Y.; Ren, W.-M.; Zhou, H.; Lu, X.-B. Development of Highly Enantioselective Catalysts for Asymmetric Copolymerization of *meso*-Epoxides and Cyclic Anhydrides: Subtle Modification Resulting in Superior Enantioselectivity. *ACS Catal.* **2019**, *9*, 1915−1922.
(22) Thevenon, A.; Garden, J. A.; White, A. J. P.; Williams, C. K. Dinuclear Zinc Salen Catalysts for the Ring Opening Copolymerization of Epoxides and Carbon Dioxide or Anhydrides. *Inorg. Chem.* **2015**, *54*, 11906−11915.
(23) Winkler, M.; Romain, C.; Meier, M. A. R.; Williams, C. K. Renewable polycarbonates and polyesters from 1,4-cyclohexadiene. *Green Chem.* **2015**, *17*, 300−306.
(24) Stößer, T.; Mulryan, D.; Williams, C. K. Switch Catalysis to Deliver Multi-Block Polyesters from Mixtures of Propene Oxide, Lactide, and Phthalic Anhydride. *Angew. Chem., Int. Ed.* **2018**, *57*, 16893−16897.
(25) Huijser, S.; Hosseini Nejad, E.; Sablong, R.; de Jong, C.; Koning, C. E.; Duchateau, R. Ring-Opening Co- and Terpolymerization of an Alicyclic Oxirane with Carboxylic Acid Anhydrides and $CO_2$ in the Presence of Chromium Porphyrinato and Salen Catalysts. *Macromolecules* **2011**, *44*, 1132−1139.
(26) Hosseini Nejad, E.; van Melis, C. G. W.; Vermeer, T. J.; Koning, C. E.; Duchateau, R. Alternating Ring-Opening Polymerization of Cyclohexene Oxide and Anhydrides: Effect of Catalyst, Cocatalyst, and Anhydride Structure. *Macromolecules* **2012**, *45*, 1770−1776.
(27) Hosseini Nejad, E.; Paoniasari, A.; Koning, C. E.; Duchateau, R. Semi-aromatic polyesters by alternating ring-opening copolymerization of styrene oxide and anhydrides. *Polym. Chem.* **2012**, *3*, 1308−1313.
(28) Inoue, S. Immortal polymerization: The outset, development, and application. *J. Polym. Sci., Part A: Polym. Chem.* **2000**, *38*, 2861−2871.
(29) Darensbourg, D. J. Chain transfer agents utilized in epoxide and $CO_2$ copolymerization processes. *Green Chem.* **2019**, *21*, 2214−2223.
(30) Hosseini Nejad, E. H.; Paoniasari, A.; van Melis, C. G. W.; Koning, C. E.; Duchateau, R. Catalytic Ring-Opening Copolymerization of Limonene Oxide and Phthalic Anhydride: Toward Partially Renewable Polyesters. *Macromolecules* **2013**, *46*, 631−637.
(31) Sanford, M. J.; Van Zee, N. J.; Coates, G. W. Reversible-deactivation anionic alternating ring-opening copolymerization of epoxides and cyclic anhydrides: access to orthogonally functionalizable multiblock aliphatic polyesters. *Chem. Sci.* **2018**, *9*, 134−142.
(32) Stößer, T.; Sulley, G. S.; Gregory, G. L.; Williams, C. K. Easy access to oxygenated block polymers via switchable catalysis. *Nat. Commun.* **2019**, *10*, 2668.
(33) Abel, B. A.; Lidston, C. A. L.; Coates, G. W. Mechanism-Inspired Design of Bifunctional Catalysts for the Alternating Ring-Opening Copolymerization of Epoxides and Cyclic Anhydrides. *J. Am. Chem. Soc.* **2019**, *141*, 12760−12769.
(34) Jeon, J. Y.; Eo, S. C.; Varghese, J. K.; Lee, B. Y. Copolymerization and Terpolymerization of Carbon Dioxide/Propylene Oxide/Phthalic Anhydride Using a (salen)Co(III) Complex Tethering Four Quaternary Ammonium Salts. *Beilstein J. Org. Chem.* **2014**, *10*, 1787−1795.
(35) Cyriac, A.; Lee, S. H.; Varghese, J. K.; Park, E. S.; Park, J. H.; Lee, B. Y. Immortal $CO_2$/Propylene Oxide Copolymerization: Precise Control of Molecular Weight and Architecture of Various Block Copolymers. *Macromolecules* **2010**, *43*, 7398−7401.
(36) Duan, Z.; Wang, X.; Gao, Q.; Zhang, L.; Liu, B.; Kim, I. Highly Active Bifunctional Cobalt-Salen Complexes for the Synthesis of Poly(ester-block-carbonate) Copolymer via Terpolymerization of Carbon Dioxide, Propylene Oxide, and Norbornene Anhydride Isomer: Roles of Anhydride Conformation Consideration. *J. Polym. Sci., Part A: Polym. Chem.* **2014**, *52*, 789−795.
(37) Burés, J. A Simple Graphical Method to Determine the Order in Catalyst. *Angew. Chem., Int. Ed.* **2016**, *55*, 2028−2031.
(38) Burés, J. Variable Time Normalization Analysis: General Graphical Elucidation of Reaction Orders from Concentration Profiles. *Angew. Chem., Int. Ed.* **2016**, *55*, 16084−16087.
(39) Grant, G. A. The many faces of partial inhibition: Revealing imposters with graphical analysis. *Arch. Biochem. Biophys.* **2018**, *653*, 10−23.
(40) Wang, Y.; Zhao, Y.; Ye, Y.; Peng, H.; Zhou, X.; Xie, X.; Wang, X.; Wang, F. A One-Step Route to $CO_2$-Based Block Copolymers by Simultaneous ROCOP of $CO_2$/Epoxides and RAFT Polymerization of Vinyl Monomers. *Angew. Chem., Int. Ed.* **2018**, *57*, 3593−3597.


https://dx.doi.org/10.1021/jacs.0c10014
*J. Am. Chem. Soc.* 2020, 142, 20161−20169